Controlled oxidative synthesis of Bi nanoparticles and emission centers in bismuth glass nanocomposites for photonic application

Shiv Prakash Singh, Basudeb Karmakar*
Glass Science and Technology Section, Glass Division, Central Glass and Ceramic Research Institute (CSIR, India), 196, Raja S.C. Mullick Road
Kolkata 700032, India.

ABSTRACT

Here we demonstrate an oxidative process to control metallic bismuth (Bi^0) nanoparticles (NPs) creation in bismuth glass nanocomposites by using $K_2S_2O_8$ as oxidant and enhanced the transparency of the bismuth glass. Formation of Bi^0 NPs has been monitored by their distinct surface plasmon resonance (SPR) band at 460 nm in the UV-visible absorption spectra. It is further confirmed by the transmission electron microscopy (TEM) images which disclose the formation of spherical Bi^0 NPs whereas the selected area electron diffraction (SAED) pattern reveals their crystalline rhombohedral phase. These glasses are found to exhibit visible and near infrared (NIR) luminescence bands at 630 and 843 nm respectively on excitation at 460 nm of the SPR band. The luminescence centers of bismuth is an ambiguous issue, however, it is reasonable to believe that the emission band at 630 nm is due to the $^2D_{5/2} \rightarrow {}^4S_{3/2}$ of Bi^0 and $^2P_{3/2}$ (1)$\rightarrow$ $^2P_{1/2}$ of Bi^{2+} transitions, and the NIR emission band at 843 nm is attributed to the $^2D_{3/2} \rightarrow {}^4S_{3/2}$ of Bi^0 transition.

Keywords: Glass, Nanocomposites, Bismuth, Photoluminescence, Electron microscopy

* To whom correspondence should be addressed. E-mail: basudebk@cgcri.res.in.

1. Introduction

In recent years, there has been an increasing interest in the synthesis of metallic nanoparticles and its surface plasmon resonance (SPR) band in the visible spectrum [1-3]. SPR band arises from the surface plasmon oscillation modes of conduction band electrons in metal nanoparticles (NPs), and strongly influences their linear and nonlinear optical response. SPR has the unique capacity to confine light in very small dimensions which could enable many new applications [1, 2]. A lot of thrusts have been given on the study of surface plasmons, local field properties of metal NPs and their potential applications in plasmonics [1]. When various applications in plasmonics are concerned, development of well controlled synthetic methodologies is the most important factors and great challenges particularly in glass matrices [2]. Exploitation of glasses as encapsulating hosts for plasmonic metal nanoparticles (fabrication of matallo-dielectric nanocomposites) provides a prospect to create a variety of nanoscale devices with attractive properties caused by amalgamation of the properties of the glass host and the nanometal. Glass present some superior inherent advantage over other dielectrics, such as high transparency, higher homogeneity than that of other sintered materials, mechanical strength, ease of fabrication in desirable size and shape, ability to withstand high intensity radiation, avoiding air oxidation of metal nanocomposites, etc. which make glasses excellent encapsulating hosts for metal NPs for practical applications [4-7].

There is a renewed interest in the bismuth glasses due to many reasons, some of them are indicated below. Bismuth glass is one of the most important amongst the heavy metal oxide (HMO) glasses due to their several inherent properties such as high refractive index, wide transmission window, broad band near infrared (NIR) luminescence, etc [8-

11]. In recent time, bismuth glasses have attracted attention of various researchers as a very important optical material from the view point of its photoluminescence properties for photonics and optoelectronic applications. In bismuth glass, the various sub-valence states of bismuth such as Bi^{5+}, Bi^{3+}, Bi^{2+}, Bi^{+} and Bi^{0} are coexist [8]. Therefore, the emission centers due to various bismuth ions are controversial issue and need further investigation.

However, bismuth oxide glasses are usually obtained in dark-brown or black color, which deepens with increasing Bi_2O_3 content and when melted above 1000^0C [9, 10]. This limits to a great extent the application of bismuth oxide glasses for optical and photonic purposes. Therefore, controlled synthesis of bismuth (Bi^0) nanoparticles (NPs) in bismuth glasses and colorless bismuth glasses are very important both academically as well as technological point of views. In our previous work [12], we have demonstrated the controlled synthesis of Bi^0 NPs in bismuth glass using $KClO_4$ and KNO_3 oxidants. To the best of our knowledge, there is no previous report on the control synthesis of Bi^o NPs in bismuth glasses by applying the oxidation technique using $K_2S_2O_8$.

In view of above and extension of our previous work [12], in this paper we report the synthesis of Bi^o NPs in the B_2O_3-ZnO-Bi_2O_3-SiO_2-K_2O glass system by controlling the auto-thermo reduction of Bi_2O_3 using $K_2S_2O_8$ as oxidizing agent and evaluation of their properties by UV-Vis spectroscopy, transmission electron microscopy (TEM), selected area electron diffraction (SAED) analysis and luminescence measurement.

2. Experimental section

Glass samples were synthesized by conventional melting and quenching techniques as described in our previous work [12], using bismuth trioxide, Bi_2O_3 (Loba Chemie), boric acid, H_3BO_3 (Loba Chemie), zinc oxide, ZnO (Loba Chemie), potassium carbonate, K_2CO_3 (Loba Chemie), silicon dioxide, SiO_2 (Bremthaler/Quarzitwerk) and potassium peroxodisulphate, $K_2S_2O_8$ (Merck) as raw materials. The raw materials for 25 g glass of composition (mol %): $32.32B_2O_3$-33.47ZnO-$11.44Bi_2O_3$-$17.74SiO_2$-$(5.03–x)K_2O$-$xK_2S_2O_8$, where x is the equivalent amount of K_2O obtained from the source of $K_2S_2O_8$ (where x is 0, 0.0011, 0.0026, 0.0053, 0.0110 and 0.0158). All the melting and annealing conditions were same as previous work [12]. Samples of 2 ± 0.01 mm thickness were prepared by cutting, grinding and polishing for optical measurements.

The UV-Vis absorption spectra in the range of 350-700 nm were recorded using a double beam UV-visible spectrophotometer (Lambda 20, Perkin-Elmer) at an error of $\pm$0.1 nm. The fluorescence spectra were measured for all the samples at an error of $\pm$0.2 nm with a Perkin Elmer Luminescence Spectrophotometer (Model LS55) exciting at 460 nm using a Xenon lamp as the excitation source and a photomultiplier tube (PMT) as detector. The TEM and SAED images were taken using a FEI instrument (Tehnai-30, ST G^2) operating at an accelerating voltage of 300 kV.

3. Results and discussion

The major problem for preparation of bismuth containing transparent glasses is the graying or blackening when melted above 1000^0C. The intensity of graying or

blackening increases with increase in melting temperature as well as Bi_2O_3 content. It is due to auto-thermo reduction of Bi^{3+} ions to bismuth metal (Bi^0) during the course of melting process. The reduction of Bi_2O_3 occurs through the following thermal decomposition reaction [9, 10]

$$2Bi_2O_3 \leftrightarrow 4Bi^0 + 3O_2 \uparrow \quad (1)$$

In the above equilibrium reaction, the metallic Bi^0 is formed with the release of oxygen. When the strong oxidizing agent, such as $K_2S_2O_8$, is added as a source of K_2O in the glass composition, it increases the oxygen partial pressure as a result of its thermal decomposition during melting process as follow [13]

$$K_2S_2O_8 \rightarrow K_2O + 2SO_3 \uparrow + \tfrac{1}{2} O_2 \uparrow \quad (2)$$

$$2SO_3 \rightarrow 2SO_2 \uparrow + O_2 \uparrow \quad (3)$$

Therefore, the reaction of the Eq. (1) proceeds in the reverse direction due to reactions of the Eqs. (2) and (3). In our previous work [12], we have used $KClO_4$ and KNO_3 as oxidants to suppress the formation of Bi^0 NPs in these glasses. By comparing the standard reduction potentials [14] as listed in Table 1**,** it is clear that the standard potential of $S_2O_8^{2-}/SO_4^{2-}$ is much higher (2.01 V) than that of Bi^+/Bi^o (0.50 V), Bi^{3+}/Bi^o (0.31 V), Bi^{3+}/Bi^+ (0.20 V) and Bi^{3+}/Bi^{2+} (<0.20 V) species, so it easily favors the backward reactions of the Eq. (1) and suppressed the auto-thermo decomposition of Bi_2O_3. It results the controlled formation of Bi^o NPs and the glasses gradually become

more transparent with well defined Bi^o SPR band with increasing $K_2S_2O_8$ concentration. This fact could be visualized clearly by the remarkable changes in the transparency of the resultant glasses as shown in Fig. 1. As the reduction potentials of various valence states of bismuth are very close to each other, therefore, it is very difficult to predict which valence state of bismuth ion will form during melting process.

The UV-Vis absorption spectra of bismuth glasses are shown in Fig. 2. The broad absorption band at 460 nm is due to the surface plasmon resonance (SPR) of Bi^o NPs. The SPR is a characteristic of metal nanoparticles embedded in a dielectric host and is attributed to the collective oscillation of electrons in response to optical excitation. The SPR of a spherical particle gives an absorbance band centered at a wavelength, λ, which can be expressed by the relation [15]

$$\lambda^2 = 4\pi^2 c^2 m_o \varepsilon_o (\varepsilon_m + 2n_o^2) / Ne^2 \qquad (4)$$

where c is the velocity of light, m_o is the charge carrier particle mass, N is the charge carrier particle concentration, e is the charge of the electron, ε_m is the optical dielectric function of the metal, n_o is the refractive index (RI) of the host material and ε_o is the free-space permeability.

ω_d is the damping frequency, which is related to the mean free path of the conduction electrons (R_{bulk}) and ν_f is the velocity of electrons at the Fermi energy. The most important parameter affecting ω_d is the particle size and it can be represented by the following equation [16]

$$\omega_d = \nu_f / R_{bulk} \quad (5)$$

It can be seen from Eq. 5 that a decrease in particle size leads to an increase in ω_d, which is causing the band to broaden and the maximum intensity to decrease.

From the Eq. 4, it is clear that the absorbance band position proportionate directly to the RI of the host material. Wang *et al.* [16] have synthesized poly (vinylpyrroldone) (PVP) stabilized bismuth nanoparticles (NPs) and found absorption peak at 281 nm associated with Bi^0 NPs. Gutiérrez *et al.* [17] have prepared nanometer-sized particles of bismuth by the radiolytic reduction of aqueous solutions of bismuth perchlorate. They observed absorption spectrum of colloidal bismuth at 253 nm. Corain *et al.* [1] have reported the absorbance band of Bi^o NPs in the host water (RI = 1.33) around 400 nm. Recently, some studies have carried out for the absorption band of metallic bismuth in various glass matrices [19-21]. Peng *et al.* [18] have found a broad absorption peak at around 465 nm for Bi_2O_3 contained glasses and assigned the peak as SPR of metallic bismuth. Romanov *et al.* [19] have observed two broad absorption peaks at 475 nm and 443 nm for two different glasses of bismuth borate and bismuth potassium phosphate glass respectively. They designated the peaks as the absorption due to metallic bismuth. Bishay [20] observed similar broad absorption at 515 nm due to elementary Bi in bismuth borate glass after γ –irradiation.

In this study, the glass has higher RI (1.76) and shows an absorption band at 460 nm. From above discussion, it is clear that the absorption at 460 nm is due to metallic bismuth nanoparticles [1, 18-20]. Khonthon *et al.* [11] and Singh *et al.* [12] have also reported such absorption band of Bi^0 NPs at 460 nm in the different glass matrices, which is analogous to this result. The absorption band of the base glass has shown in the

inset of the Fig. 2. The base glass is black and has a very weak signature of SPR band. On the other hand, when 0.0011 mol % of $K_2S_2O_8$ has added as a source of K_2O to the base glass, the surface plasmon band has materialized very distinct. The intensity of SPR band gradually decreases with addition of further amount of $K_2S_2O_8$ (up to 0.0158 mol %) and finally the band weaken. However, the SPR band position remains unchanged at 460 nm in all the cases because of constancy of RI and glass composition. These significant effects of $K_2S_2O_8$ are shown in the Fig. 2. Addition of $K_2S_2O_8$ as a source of K_2O leads to the controlled generation of Bi^0 NPs and elimination of graying or blackening of bismuth glasses to colorless.

The TEM image of glass in which $K_2S_2O_8$ is not being used as a source of K_2O has been shown in Fig. 3. It reveals huge and densely embedded Bi^0 NPs of spherical shape with size range 2-5 nm. The SAED pattern of this glass shows no any distinct pattern. This would be due to presence of very small size of Bi^0 NPs. The glass containing 0.0026 mol % of $K_2S_2O_8$ shown in the Fig. 4, demonstrated the presence of comparatively less amount of spherical Bi^0 NPs ranges 10-12 nm. Whereas its SAED depicts the clear patterns of <012> and <104> *hkl* planes of rhombohedral Bi nanometallic particles, which have been identified from the d-spacing (JCPDS File Card No.: 85-1330). Wang *et al.* [16] have demonstrated to control the size of Bi nanoparticles in the range 6-13 nm by adjusting the molar ratio of PVP to $BiCl_3$ or the concentration of $BiCl_3$. Son *et al.* [21] have developed a simple synthetic route by reduction of bismuth thiolate to uniform-sized rhombohedral Bi nanocrystals with controlled particle sizes ranging from 6 to 27 nm.

Photoluminescence emission on excitation at the SPR band of nanosized bismuth particles has not been reported previously and thus it is very interesting to study its various emission centers. The red and NIR photoluminescence emission of the bismuth glass without and with oxidizing agent $K_2S_2O_8$, excited by SPR band at 460 nm are shown in Fig. 5 (A). Its excitation spectra have also been shown in Fig. 5 (B) for conformation of the origin of luminescence. When excited at 460 nm, strong emission bands are observed in visible region around 630 nm and in the NIR region around 843 nm. It observed first that the intensity of emission bands at 630 nm decreases at 0.0011 mol % containing $K_2S_2O_8$ glasses. But further gradually increases up to 0.0053 mol % of $K_2S_2O_8$ and then again decreases at higher concentrations of $K_2S_2O_8$ (Fig. 6). However, the intensity of the emission band at 843 nm, first gradually increases from 0 to 0.0053 mol % and then decreases with higher concentration of $K_2S_2O_8$ (Fig. 7).

Bismuth has several kinds of valence states existing simultaneously in glasses and its crystalline compounds. The various emission centers in the bismuth glass arise due to various ionic species of bismuth (e.g., Bi^{3+}, Bi^{2+} and Bi^{+}). The formation of various valence state of bismuth take place by the auto-thermo reduction of Bi^{3+} ions (origin is raw material, Bi_2O_3) proceeds towards Bi^0 reversibly during melting process and forming the following intermediate valence states:

$$Bi^{3+} \leftrightarrow Bi^{2+} \leftrightarrow Bi^{+} \leftrightarrow Bi^{0} \qquad (6)$$

It is not clear that which valence of bismuth ion contributes to the various emissions up to now. Some reports of Zhou *et al.* [8], Steensel *et al.*[22] and others [23, 24] have reported

the typical luminescence spectra of Bi^{3+} centered in the blue to green region when excited in the UV region. Therefore, the emission bands observed in this study, centered at 630 and 843nm could not be due to Bi^{3+} ion. The luminescence center might be due to the other low valence state species of Bi, such as Bi^{2+}, Bi^{+} or Bi^{0}. Zhou *et al.* [8], have observed visible orange-red emission centered at 590 nm attributed to $^2P_{3/2} \rightarrow {}^2P_{1/2}$ transition of Bi^{2+} when excited at 280 and 483 nm for different samples. Hamstra *et al.* [25] have suggested the red luminescence due to Bi^{2+} ion, varying in the range of 16.0 to 17.1 (x 10^3) cm^{-1} in the various host lattices. They have shown the luminescence of $BaSO_4$: Bi^{2+} at 625 nm when excited at 455 nm. Ren *et al.* [26] have shown the visible luminescence spectra excited at wavelength range from 400 to 650 nm. The observed luminescence, when excited within this range, consists of two bands centered between 650 and 760 nm, respectively. They assigned this red luminescence as characteristic spectra of Bi^{2+}. Such red luminescence and the absorption bands arise from the electron transition between the first excited level $^2P_{3/2}$ and ground level $^2P_{1/2}$ of Bi^{2+}. Because the absorption band observed by them is about 500 nm and the red luminescence from the glass are almost the same with the absorption and luminescence from Bi^{2+} activated crystals. They have ascribed this peak to the electron transition $^2P_{1/2} \rightarrow {}^2P_{3/2}$ and $^2P_{3/2} \rightarrow {}^2P_{1/2}$, respectively, of Bi^{2+}.

The excitation-wavelength-dependent NIR emission centered found by the Zhou *et al.* [8] at 1100 and 1400 nm are assigned to the Bi^{+} when exited at 532 and 800 nm respectively with longer decay time. Meng *et al.* [27] has also shown the possibility of $^3P_2 \rightarrow {}^3P_0$ transition due to Bi^{+} ion in the NIR region. Qiu *et al.* [28] have ascribed the infrared emissions in Bi-doped multi-component glass is due to $^3P_1$ to $^3P_0$ transition of

Bi^{+}. Ren *et al.* [27] have discussed about the infrared luminescence excited at 700, 800, and 980 nm which have ascribed to the electronic transition $^{3}P_{1}$ to $^{3}P_{0}$ of Bi^{+} ions in distinct sites. Peng *et al.* [29] have demonstrated NIR emission, centered at around 1250 nm in the BBSPS glasses, upon optical excitation at 785 nm and this emission center ascribed to Bi^{+} species. They have demonstrated different mechanism for the NIR emission in Bi-doped glasses. They have also reported the NIR absorption and emission properties of bismuth glass and their dependence on the melting temperature. The dependence of absorption and NIR emission of bismuth glasses on the melting temperature has interpreted as thermal dissociation of Bi_2O_3 into metallic Bi. Darkening of bismuth glass melted at $1300^{0}C$ is because of the agglomeration of metallic Bi nanoparticles. Romanov *et al.* [19] have reported about the NIR luminescence due to univalent Bi^{+} in borate and phosphate glasses. Peng *et al.* [18] have observed five absorption band in Bi-doped germanate glass around 320, 500, 700, 800 and 1000 nm which are assigned to Bi^{0} transitions $^{4}S_{3/2} \rightarrow ^{2}P_{3/2}$, $^{4}S_{3/2} \rightarrow ^{2}P_{1/2}$, $^{4}S_{3/2} \rightarrow ^{2}D_{5/2}$, $^{4}S_{3/2} \rightarrow ^{2}D_{3/2}(2)$ and $^{4}S_{3/2} \rightarrow ^{2}D_{3/2}$ (1), respectively, and broadband NIR emission is assigned to the transition $^{2}D_{3/2}(1) \rightarrow ^{4}S_{3/2}$.

Taking into account all the above arguments, our results are well matched with the energy levels of Bi^{0} which was explained by Peng *et al.* [18] and the emission bands at 630 nm and 843 nm could be assigned to electron transition $^{2}D_{5/2} \rightarrow ^{4}S_{3/2}$ and $^{2}D_{3/2} \rightarrow ^{4}S_{3/2}$ of Bi^{0} respectively. But, in our experiment, we have found that the glass, which has not contained oxidizing agent $K_2S_2O_8$ has shown maximum emission band at 630 nm. This maximum intensity is due to $^{2}D_{5/2} \rightarrow ^{4}S_{3/2}$ transition of Bi^{0} which is present in huge amount in the glass. After addition of 0.0011 mol % of $K_2S_2O_8$ in the glass, the

emission band intensity decreases, and this is due to the dramatically decrease of Bi^0 in the glass. When further addition of $K_2S_2O_8$ (0.0026 and 0.0053 mol %) results the decrease in Bi^0 in the glass (Fig. 6). But, surprisingly, the emission intensity has not further reduced. The intensity increases with the broadening of emission band at 630 nm. This observation indicates the probability of energy transfer from the Bi^0 to other luminescent center or formation of different valence state of bismuth. From the previous discussion, it has revealed that the emission in this red region is arises due to $^2P_{3/2}$ (1) → $^2P_{1/2}$ transition of Bi^{2+} species which is also well agreement with the conclusion drawn by Hamstra *et al.* [29] in their experiment. Therefore, it could be possible that $K_2S_2O_8$ suppressed the forward reduction reaction of Eq. 6 gradually and which leads to the enhancement of the emission intensity. The broadening of the emission band may be due to the presence of multiple emission bands of Bi^0 and Bi^{2+} and which can be visualize from the deconvoluted spectrum as shown in the inset of Fig. 5 (A). This phenomenon can be well understood by the energy diagram [8, 18] as shown in the Fig. 8. The further decrease in the intensity attributed to the concentration quenching of Bi^{2+} ions due to the gradual increase in formation of Bi^{2+} in the glass host.

The observed NIR emission at 843 nm is gradually increases with the concentration of $K_2S_2O_8$ up to 0.0053 mol %, and further decreases (at 0.0110 and 0.0158 mol %). The profile of the emission band is similar in all the cases. It is seen from the previous discussion [8, 23, 28], some of researchers have suggested the NIR emission band is due to Bi^+ ionic species. But Peng *et al.* [18, 30] have ascribed the NIR emission band to Bi^0 species. Here, in this study, the NIR band at 843 nm is found to well match with the proposed energy levels of Bi^0 by Peng *et al.* [30] and is attributed to $^2D_{3/2}$→$^4S_{3/2}$

transition (Fig. 8). The gradual increase of emission intensity (Fig. 7) is attributed to increase in inter atomic distance between the bismuth nanoparticles to the critical distance [31, 32]. Further exceed in inter-atomic distance than the critical distance results the decrease in the luminescence.

4. Conclusions

In summary, the dependence of absorption and emission spectra in the visible as well as NIR region due to various valance states of bismuth on the oxidizing agent $K_2S_2O_8$ has been deduced here. There is no any such previous report on the oxidant dependent controlled generation of bismuth nanoparticles, surface plasmon resonance, and its photoluminescence property. The UV-visible absorption spectra show the characteristic invariable SPR band of Bi^0 NPs at 460 nm. TEM images and SAED pattern confirm the formation of spherical shaped rhombohedral Bi^0 nanoparticles. Very significant emission centers due to Bi^0 and Bi^{2+} have been observed at 630 and 843 nm when excited at SPR wavelength. We believe that this work will create a new vista for photonics and optoelectronic research.

Acknowledgements

SPS express his sincere gratitude for the financial support of the Council of Scientific and Industrial Research (CSIR), New Delhi in the form of CSIR-SRF under the sanction number 31/15(78)/2010-EMR-I. The authors thank Director of the institute for his kind permission to publish this paper. They also thankfully acknowledge the Electron Microscope Division of this institute for recording the TEM, and SAED images.

References

[1] B. Corain, G. Schmid, N. Toshima (Eds.), Metal Nanoclusters in Catalysis and Materials Science: The Issue of Size Control, Elsevier, Amsterdam, 2008.

[2] F. Gonella, P. Mazzoldi, Metal Nanocluster Composite Glasses. in: H. S. Nalwa, Ed. Handbook of Nanostructured Materials and Nanotechnology; 4th Vol., Academic Press, London, 2000 p. 81.

[3] P. Mulvaney, Langmuir 12 (1996) 788-800.

[4] B. Karmakar, T. Som, S. P. Singh, M. Nath, Trans. Ind. Ceram. Soc. 69 (2010) 171-186.

[5] S. Chen, T. Akai, K. Kadono, T. Yazawa, Appl. Phys. Lett. 79 (2001) 3687-3689.

[6] H. Zeng, G. Chen, J. Qui, X. Jiang, C. Zhu, F. Gan, J. Non-Cryst. Solids 354 (2008) 1155-1158.

[7] L. R. P. Kassab, K. J. Plucinski, M. Piasecki, K. Nouneh, I. V. Kityk, A. H. Reshak, R. de A. Pinto, Opt. Commun. 281 (2008) 3721–3725.

[8] S. Zhou, N. Jiang, B. Zhu, H. Yang, S. Ye, G. Laksminarayana, J. Hao, J. Qiu, Adv. Funct. Mater. 18 (2008) 1407-1413.

[9] Y. Zhang, Y. Yang, J. Zheng, W. Hua, G. Chen, J. Am. Ceram. Soc. 91 (2008) 3410-3412.

[10] O. Sanz, E. Haro-Poniatowski, J. Gonzalo, J. M. Fernández Navarro, J. Non-Cryst. Solids 352 (2006) 761-768.

[11] S. Khonthon, S. Morimoto, Y. Arai, Y. Ohishi, Opt. Mater. 31 (2009) 1262-1268.

[12] S. P. Singh, B. Karmakar, Mater. Chem. Phys. 119 (2010) 355–358.

[13] J. W. Mellor, Comprehensive Treatise on Inorganic and Theoretical Chemistry. Vol. IX, Longmans, London, 1947, p. 616.

[14] P. Vanýsek, Electrochemical Series. In: D. R. Lide, Ed., CRC Hand Book of Chemistry and Physics, p. 22 (CRC Press, 1994).

[15] P. D. Persans and K. L. Stokes Embedded Nanocrystal Spectroscopy: Semiconductor and Metal Particles in Insulators. in: A. N. Goldstein, Ed. Handbook of Nanophase materials, Marcel Dekker, New York, 1997, p. 271.

[16] Y. W. Wang, B. H. Hong, K. S. Kim, J. Phys. Chem. B 109 (2005) 7067-7072.

[17] M. Gutiérrez, A. Henglein, J. Phys. Chem. 100 (1996) 7656-7661.

[18] M. Peng, C. Zollfrank, L. Wondraczek, J. Phys.: Condens. Matter. 21 (2009) 285106 1-6.

[19] A. N. Romanov, Z. T. Fattakhova, D. M. Zhigunov, V. N. Korchak, V. B. Sulimov, Opt. Mater. 33 (2011) 631–634.

[20] A. Bishay, Phys. Chem. Glasses 2 (1961) 33–38.

[21] J. S. Son, K. Park, M.-K. Han, C. Kang, S.-G. Park, J.-H. Kim, W. Kim, S.-J. Kim, T. Hyeon, Angew. Chem. Int. Ed. 50 (2011) 1363 –1366.

[22] L. I. van Steensel, S. G. Bokhove, A. M. van de Craats, J. de Blank, G. Blasse, Mater. Res. Bull. 30 (1995) 1359-1362.

[23] M. Peng, B. Wu, N. Da, C. Wang, D. Chen, C. Zhu, J. Qiu, J. Non-Cryst. Solids 354 (2008) 1221-1225.

[24] M. Xiang-Geng, P. Ming-Ying, C. Dan-Ping, Y. Lv-Yun, J. Xiong-Wei, Z. Cong-Shan, Q. Jian-Rong, Chin. Phys. Lett. 22 (2005) 615-617.

[25] M. A. Hamstra, H. F. Folkerts, G. Blasse, J. Mater. Chem. 4(8) (1994) 1349-1350.

[26] J. Ren, G. Dong, S. Xu, R. Bao, J. Qiu, J. Phys. Chem. A 112 (2008) 3036-3039.

[27] X. Meng, J. Qiu, M. Peng, D. Chen, Q. Zhao, X. Jiang, C. Zhu, Opt. Exp. 13 (2005) 1635-1642.

[28] J. Qiu, M. Peng, J. Ren, X. Meng, X. Jiang, C. Zhu, J. Non-Cryst. Solids 354 (2008) 1235-1239.

[29] M. Peng, Q. Zhao, J. Qiu, L. Wondraczek, J. Am. Ceram. Soc. 92 (2009) 542-545.

[30] M. Peng, B. Sprenger, M. A. Schmidt, H. G. L. Schwefel, L. Wondraczek, Opt. Exp. 18 (2010) 12852-12863.

[31] Y. C. Chang, C. H. Liang, S. A. Yan, Y. S. Chang, J. Phys. Chem. C, 114, (2010) 3645–3652.

[32] H. S. Yoo, S. Vaidyanathan, S. W. Kim, D. Y. Jeon, Opt. Mater. 31 (2009)1555–1558.

Figure captions

Fig. 1. (Color online) Photograph is of the polished glasses (thickness = 2 mm and identifiable by their bottom letters) using (a) 0, (b) 0.0011, (c) 0.0026, (d) 0.0053, (e) 0.0110 and (f) 0.0158 mol % of $K_2S_2O_8$ laid on black lines to show their transparency to the naked eye.

Fig. 2. Absorbance spectra of glasses using (a) 0 (inset), (b) 0.0011, (c) 0.0026, (d) 0.0053, (e) 0.0110 and (f) 0.0158 mol % of $K_2S_2O_8$.

Fig. 3. TEM image and SAED pattern of the glass without using $K_2S_2O_8$.

Fig. 4. TEM images and SAED pattern of the glass using 0.0026 mol % of $K_2S_2O_8$.

Fig. 5. (Color online) (A) Photoluminescence emission and its (B) excitation spectra of glasses using (a) 0, (b) 0.0011, (c) 0.0026, (d) 0.0053, (e) 0.0110 and (f) 0.0158 mol % of $K_2S_2O_8$ when excited at 460 nm. The deconvoluted spectrum of (c) is shown in the inset of (A).

Fig. 6. Photoluminescence (PL) emission intensity at 630 nm as a function of $K_2S_2O_8$ concentration (mol %) when excited at 460 nm.

Fig. 7. Photoluminescence (PL) emission intensity at 843 nm as a function of $K_2S_2O_8$ concentration (mol %) when excited at 460 nm.

Fig. 8. Schematic energy level diagrams of Bi^{2+} and Bi^{0} centers.

Table 1
Redox reaction and reduction potential of peroxodisulphate and bismuth ions

Redox reaction	Reduction potential (E^o, V)
$S_2O_8^{2-} + 2e^- = 2SO_4^{2-}$	2.01
$Bi^+ + e^- = Bi^o$	0.50
$Bi^{3+} + 3e^- = Bi^o$	0.31
$Bi^{3+} + 2e^- = Bi^+$	0.20
$Bi^{3+} + e^- = Bi^{2+}$	< 0.20[a]

[a] Exact value is not available

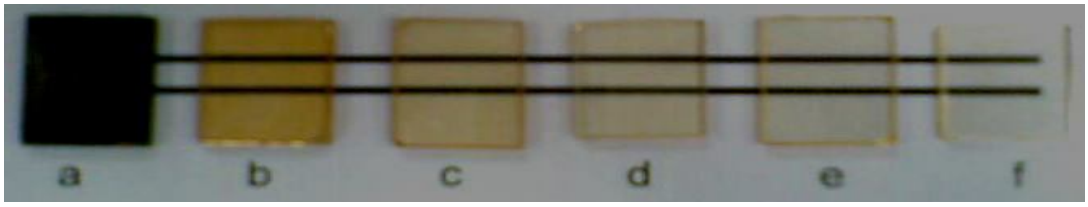

Fig. 1. (Color online) Photograph is of the polished glasses (thickness = 2 mm and identifiable by their bottom letters) using (a) 0, (b) 0.0011, (c) 0.0026, (d) 0.0053, (e) 0.0110 and (f) 0.0158 mol % of $K_2S_2O_8$ laid on black lines to show their transparency to the naked eye.

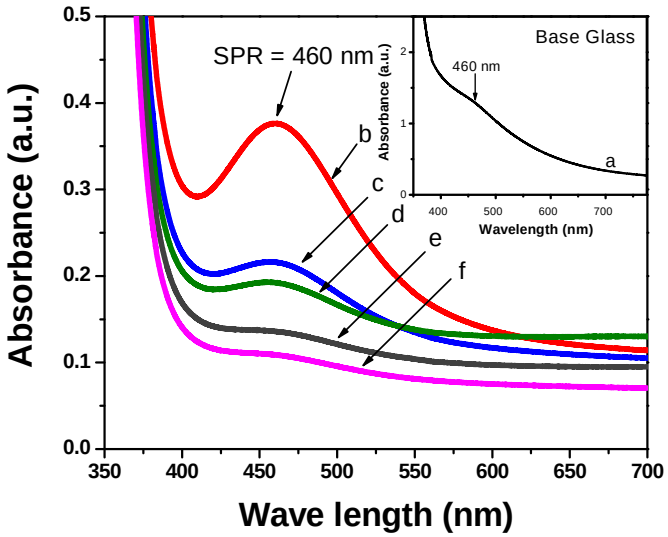

Fig. 2. (Color online) Absorbance spectra of glasses using (a) 0 (inset), (b) 0.0011, (c) 0.0026, (d) 0.0053, (e) 0.0110 and (f) 0.0158 mol % of $K_2S_2O_8$.

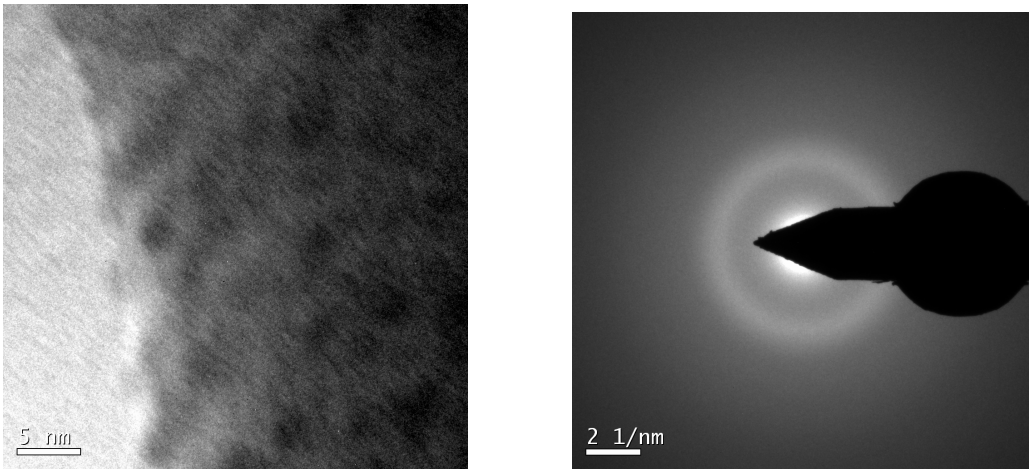

Fig. 3. TEM image and SAED pattern of the glass without using $K_2S_2O_8$.

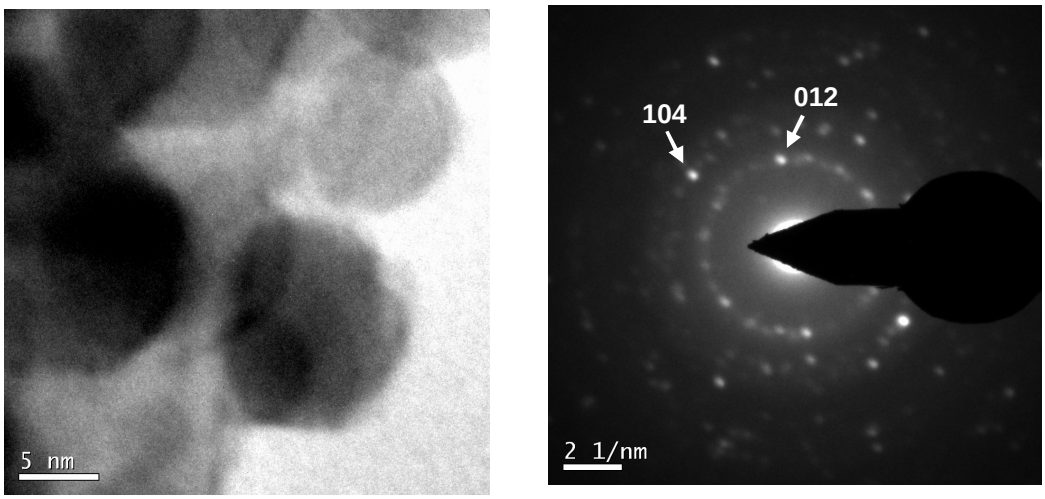

Fig. 4. TEM images and SAED pattern of the glass using 0.0026 mol % of $K_2S_2O_8$.

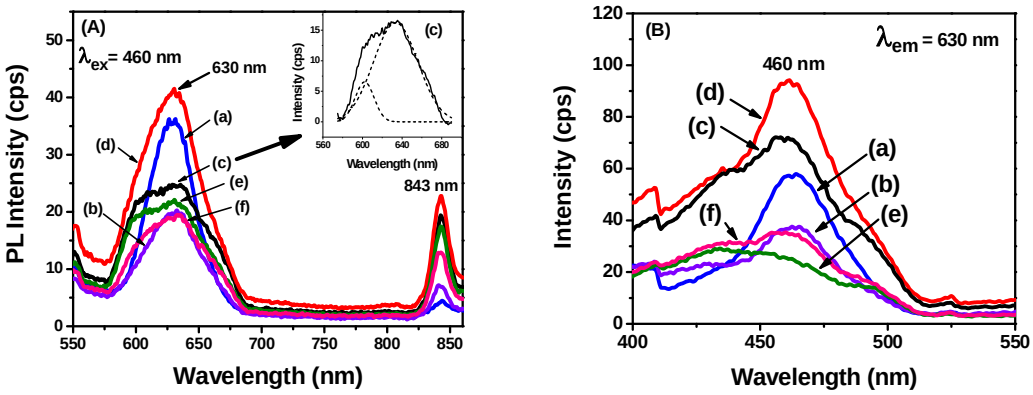

Fig. 5. (Color online) (A) Photoluminescence emission and its (B) excitation spectra of glasses using (a) 0, (b) 0.0011, (c) 0.0026, (d) 0.0053, (e) 0.0110 and (f) 0.0158 mol % of $K_2S_2O_8$ when excited at 460 nm. The deconvoluted spectrum of (c) is shown in the inset of (A).

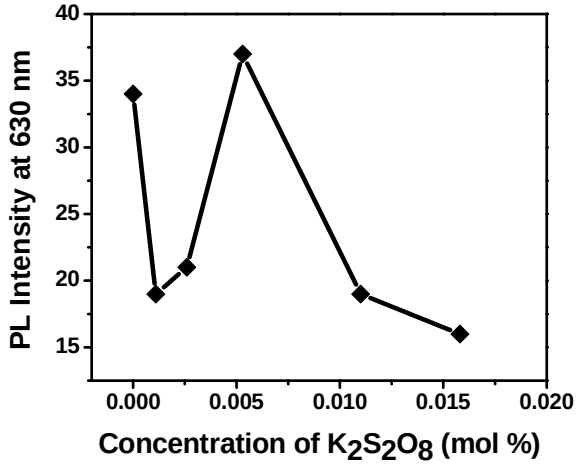

Fig. 6. Photoluminescence (PL) emission intensity at 630 nm as a function of $K_2S_2O_8$ concentration (mol %) when excited at 460 nm.

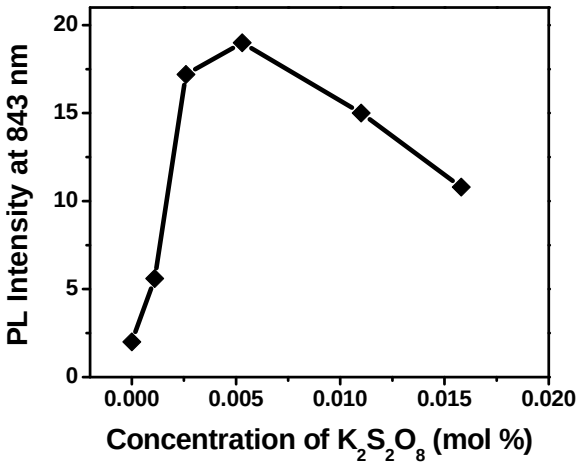

Fig. 7. Photoluminescence (PL) emission intensity at 843 nm as a function of $K_2S_2O_8$ concentration (mol %) when excited at 460 nm.

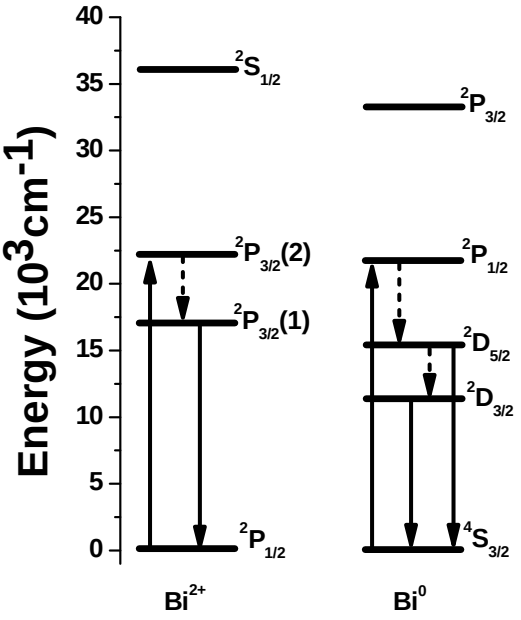

Fig. 8. Schematic energy level diagrams of Bi^{2+} and Bi^0 centers.